Characterization of a precision modular sine wave generator

J. Kučera[1,2], J. Kováč[1,2], L. Palafox[3], R. Behr[3], L. Vojáčková[1]

[1] Czech Metrology Institute (CMI), Okružní 31, 638 00 Brno, Czech Republic
[2] Czech Technical University in Prague (CTU), FEE, Department of Measurements, Technická 2, 166 27 Prague 6, Czech Republic
[3] Physikalisch-Technische Bundesanstalt, Bundesallee 100, 38116 Braunschweig, Germany

E-mail: jkucera@cmi.cz

Abstract

In this paper we describe the properties of a precision modular sine wave generator, initially developed at CMI for an application in electrical ratio impedance bridges. It operates up to 7 Vrms in the frequency range from mHz up to 20 kHz, extendable to 100 kHz with small changes to the filters. The generator went through several development loops dealing with amplitude and phase accuracy, linearity, absolute amplitude stability, amplitude ratio stability, and others. It has been used in metrology applications dealing with target relative uncertainties down to 10^{-8} level. Here, we collect and discuss experimental results in context with target applications, which may be of interest for metrologists working not only in the field of AC impedance metrology but in on-site comparisons of AC quantum voltage standards based on AC Josephson effect and where is a need of precision voltage sources generally too.

Keywords: signal generator, synthesizer, voltage, calibration, metrology, impedance, AC Josephson effect

1. Introduction

Sine wave voltage generators play an essential role in many electrical measurements, where they serve as a measuring or an energizing signal source. For primary metrology purposes in audio frequency range, the specifications of such voltage sources require exceeding the properties of commercially available generators, e.g., for various types of impedance bridges [1], where high stability, high resolution, low inter-channel crosstalk, and external references are crucial. Limitations of such generators for impedance metrology were investigated [2]. A need to go beyond specifications of series produced commercial generators led to development of dedicated techniques, where improved stability or resolution of output signals was achieved, e.g. [3], [4], distortion of sinewave was lowered, e.g. [5], or programmable Josephson arrays were applied to lower uncertainty of AC voltage ratio, e.g. [6].

A universal ultra-stable sine wave generator (SWG) with high amplitude and phase resolution, operating from mHz to tens of kHz, and optimized especially for the audio frequency range was developed in recent years at CMI. Combining advanced electronics with an optimized design, a digital direct synthesis (DDS) based modular generator with two output channels in each compact module with stability level below 0.1 μV/V within one hour, a resolution better than 0.01 μV/V of 7 Vrms full

scale (FS) – i.e. 20 Vpp –, a programmable refining of spurious-free dynamic range (SFDR), internal/external clock and internal/external reference voltage was developed. A built-in compact option for battery operation lowers the noise coupling from the power source net and omits grounding loops for the most sensitive measurements. Such a generator can be applied in circuits dedicated for measurements of two or four-terminal pair [7] defined electrical impedance standards. High universality and precision of generators have been demonstrated during the development of digital impedance ratio bridges dedicated for primary impedance metrology, where various types of loads are present [8], [9]. The suitability of generators for applications with sensitive devices has been demonstrated during the development of circuits energized from generators and including the quantum Hall effect based resistance standards too [10], [11]. Moreover, its applicability as a transfer standard for AC quantum voltmeter comparisons has been recently tested. This paper gives an overview about the development and properties of the generator.

2. Basic properties

An outline of the first generator version was given in [8]. General properties of the latest generator revision are summarized in Table I, the updated and detailed description follows.

The basic module of the generator is a two-channel voltage source that can be powered from mains power or with an optional full electrical isolation. It can be operated in two modes:

- individually from a simple USB to optic fiber converter,
- in connection with a control unit (SCU) for up to four modules, which contains the USB to optic fiber cable converter, a clock distribution network, and the charger for the batteries. Up to eight signal channels can be operated simultaneously from a single computer program today. Further extension is possible with appropriate modifications.

TABLE I
PROPERTIES OF THE SWG GENERATOR

Characteristic	Value
Max. output voltage (FS)	7 V_{rms}
Max. output current	170 mA
Amplitude resolution	< 0.01 μV/V of FS
Phase resolution	2×10^{-7} rad
Absolute voltage stability	Up to 0.05×10^{-6}/30 min.
Rel. voltage ratio stability of chan. A/B	Up to 0.01×10^{-6}/30 min.
Frequency range	1 mHz to 20 kHz *)
SFDR**) for sinewave 0.01 to 7 V_{rms}	> 95 dB @ 100 Hz > 85 dB @ 1 kHz
Crosstalk between channels A and B **)	< –150 dB @ 1 kHz
Crosstalk between different modules	Not measurable
Reference clock	1/10/20 MHz Ext. or Int.
DAC sampling rate	1 MHz
Reference DC voltage	10 V_{dc} Int./ 5 to 10 V_{dc} Ext.
Duration of the battery operated mode	Up to 8 hours

∗) *Optimized for kHz range. Extendable with a modification of the output filters up to 100 kHz*

∗∗) *Without sw optimization and load*

2.1 Principle of operation

The generator uses Direct Digital Synthesis (DDS) and consists mainly of a frequency reference, a field programmable gate array (FPGA), a sine wave look-up table and digital-to-analog converters (see Figure 1). The frequency reference can be selected either from an external reference clock source (input ExtCLK) or from an internal 50 MHz clock oscillator. Due to built-in frequency divider, the external clock can be driven from 1, 10 or 20 MHz TTL signal. The sine waves show very clean spectra due to the combination of the high resolution of the stored sine wave and a low clock jitter (the internal clock has a phase jitter lower than 1 ps). Instead of the preprogrammed sinewave, an arbitrary waveform can be stored in the internal memory too.

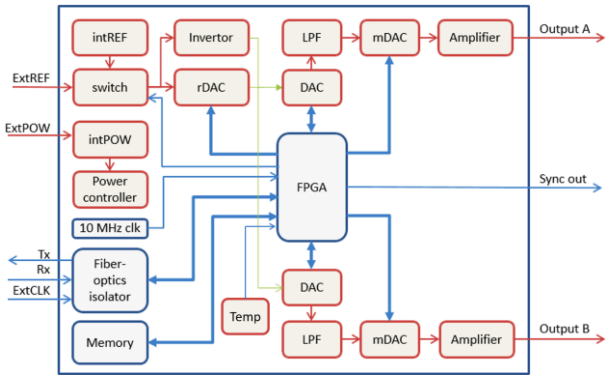

Figure 1: Diagram of the SWG generator with the red blocks related to analog signal paths and blue blocks for the digital signal paths) © 2018 IEEE. Updated reprint, with permission, from [8]).

The voltage reference of each SWG module is shared by A and B channels, thus its drift has no influence on the output voltage ratio. This is a critical property for fully digital impedance ratio bridges, which will be discussed later. The voltage reference for DACs can be selected between an internal 10 V (intREF) or a variable external (input ExtREF) reference. A temperature sensor (Temp) is implemented to monitor the environment of sensitive parts of the module.

The 20-bit digital-to-analog converter (DAC) is used to generate a pure sine wave signal with a fixed output amplitude and operates at a sampling rate of 1 MHz. A second order low pass filter (LPF) is used after the DAC to remove higher harmonics from the output signal. Then, the output amplitude of the channel is set by an 18-bit multiplying circuit (mDAC), followed by a power amplifier based on bipolar transistors. A voltage sense circuit is implemented to suppress potential effects of the output circuits on the signal amplitude.

Including mDAC as a part of the sine wave generation circuit presents the advantage of preserving a high SFDR even for extremely small output voltages. For the most critical applications, where pure sinewaves are required, a programmable refining of SFDR is implemented: higher harmonics can be reduced by combining the original signal with a phase shifted replica of the harmonics [12]. An example of improved SFDR of 976 Hz signal is given in Figure 2, where SFDR was increased from 88 to 108 dB.

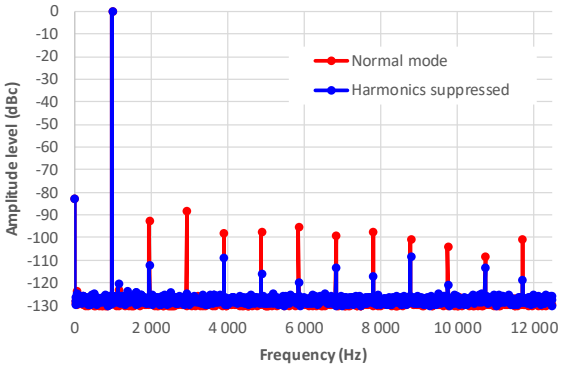

Figure 2. An example of spectrum of the generator with and without reduction of first eleven higher harmonic tones for 1 Vrms signal.

To obtain even higher output resolution than 18 bits, the DAC reference voltage can be adjusted within a small range by an additional 16-bit circuit (rDAC) for each output channel separately. A coupled control of mDAC and rDAC allows us to achieve a resolution better than 0.01 μV/V of FS. The achieved amplitude resolution of better than 0.01 μV/V of FS is a direct result of the combination of mDAC and rDAC.

The SWG generator includes several measures to protect connected devices from discontinuities in the output signal. Any changes to the output amplitude settings are performed when the signal is crossing zero voltage. Also, the phase shift change of the signal is continuous and implemented as a short time frequency sweep. The signal continuity is useful when driving inductive impedances or quantum Hall devices, where any injected charges can lead to degradation of devices. An example of the continuous behavior of a reprogrammed generator is shown in Figure 3. An external trigger circuit for a digitizer or a reference signal of lock-in amplifier can be synchronized from TTL signal (Sync out) with same frequency as the output signal. Different SWG modules can be programmed simultaneously at different frequencies.

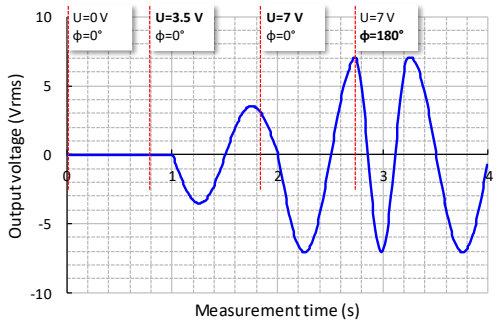

Figure 3. An example of continuous change of the output signal of frequency 1 Hz, when the amplitude and the phase is modified by a user (signal was recorded with 3458A).

The design of a two-channel module is shown in Figure 4. Except for power supply connectors, the front panel contains all controls and interface connectors. The three BPO/MUSA connectors are used for channels A, B, and an optional ground connection. Communication with the control unit or the computer is performed via fiber optic cables. An external clock reference can be connected to either a fiber optic cable or a BNC input. An external voltage reference can be connected using a BNC. The generator is powered from an external power supply (extPOW), or an integrated battery pack (intPOW) to minimize

crosstalk between SWG module and surrounding environment (e.g. coupling with other devices in the circuit via power net). An integrated switchable active air cooling of all inner parts improves the stability of the output voltage under different loads.

Figure 4. View of a SWG generator module without the top cover. Upper: front view —channel A and B outputs (left), communication and clock optical fiber cable connectors (right top), external voltage reference input (center right), status LEDs (bottom right). Lower: rear view — power supply output for custom electronics (middle), fan outlet, charger input (right).

2.2 Stability of generators

Depending on the target application, both absolute voltage stability (for voltage applications) and the ratio of two output voltages (for impedance bridges) are of interest.

2.2.1 Stability of the output voltage

The absolute output voltage stability was investigated with PTB's AC quantum voltmeter (its principle is described later in section 4). Figure 5 shows an Allan deviation analysis for three different cases. Firstly, the generator has been temperature stabilized to $\Delta T = \pm 10$ mK using an MI thermostat chamber[1]. The results show very good stability of 0.03 μV/V for measurement times of 200 – 400 s. Even after 1 hour, the Allan deviation is at the level of 0.1 μV/V. The blue curve shows a similar measurement with the SWG running in a laboratory regulated with $\Delta T = \pm 1$ K and shows comparable performance. The third case, where an external LC filter was added, is not related directly to SWG properties and is discussed later in section 4.

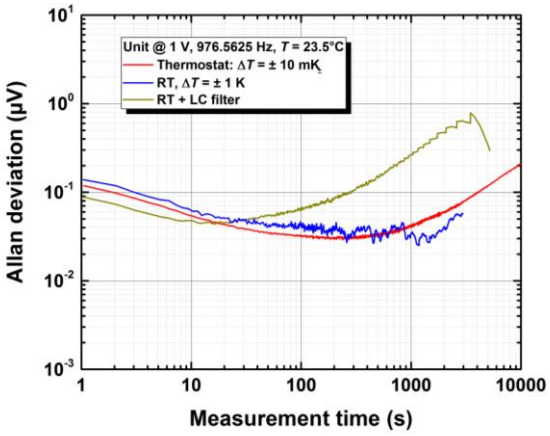

Figure 5. Allan deviation analyses for $f = 976.5625$ Hz and $V_{RMS} = 1$ V. The generator was temperature stabilized in a thermostat ($\Delta T = \pm 10$ mK) or just in a temperature-controlled laboratory ($\Delta T = \pm 1$ K). In addition, the analysis is shown when the LC filter (0.1 µF–100 nH–1.5 µF) is placed at the output of the device.

2.2.2 Stability of the voltage ratio

The stability of the output voltage ratio of channels A and B of one SWG module was investigated with a coaxial ratio voltage bridge. The reference arms were based on an inductive voltage divider and the second pair of arms was formed from channels A and B. Bridge voltage was monitored with a lock-in amplifier, synchronized with generated voltages. Figure 6 shows an Allan deviation analyses of relative ratio deviation for voltage ratio N=1:1 and N=10:1. In both cases, the level near 0.01 $\times 10^{-8}$ was achieved within 300 s and remained during the whole experiment. The total measurement time was 19 hours for the 1:1 ratio and 5 hours for the 10:1 ratio. Lock-in amplifier integration time was 10 s.

Long-term stability has been investigated by measuring the ratio between FS outputs of three different SWG modules configured with internal voltage references and at frequencies up to 2 kHz. The ratios have deviated from their averaged value by less than 6 µV/V over four years.

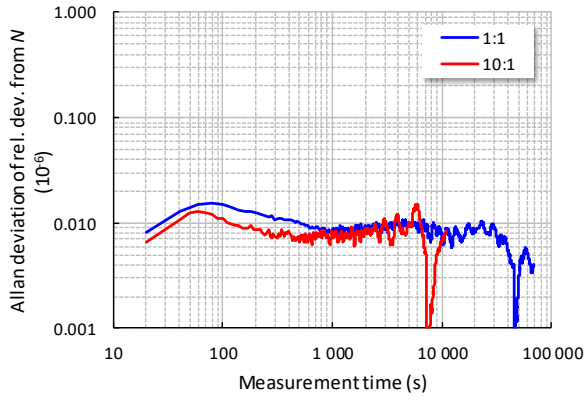

Figure 6. Allan deviation analyses of relative deviation from ratio N=1:1 and 10:1, at frequency 976 Hz. The generator was in a temperature-controlled laboratory ($\Delta T = \pm 0.5$ K).

2.3 Linearity

The linearity of generated signals is a critical property, especially for an application in fully digital impedance bridges, where the ratio of compared impedances is derived from the ratio of output voltages of the two generators. The accuracy of the ratio measurement is directly limited by the accuracy of the generated voltage signals for the reference ratio arms. In real applications, both differential and integral linearity should be known.

2.3.1 Differential nonlinearity

Beside standard linearity tests, where is involved a reference digitizer with sufficient linearity, Kucera at al. [8] introduced the idea of testing discontinuities in the output voltage transfer function (differential nonlinearities), and the phase of the generators by means of simple measurements with two generators and one lock-in amplifier. The method is focused on determining the effect of a change in the value of multiple bits on the amplitude and the phase error by evaluating the voltage difference between outputs A and B when mDAC is used to modify the output amplitude of the generator. Such testing is focused on the most significant differential nonlinearities. These occur when an increase of binary code by one LSB causes a change of multiple bits (e.g. increase from binary code 01111 to 10000).

Such a measurement was repeated with a new SWG generator, which has been recently fabricated, i.e. with electronic parts from another fabrication batch, also for the mDAC circuits. The left graph in figure 5 shows the absolute errors for the two outputs in one module in terms of LSBs, whereas the right graph shows the relative amplitude errors in µV/V of FS. New measurements (Figure 5 left) produced similar results (compare with Figure 8 in [8]). The absolute quadrature error E_Y significantly raises for bits higher than m=10. Nevertheless, the in-phase amplitude raises with more significant bits faster too. Thus, the effect of E_Y on the amplitude error is finally small, lower than 1 µV/V of FS at tested points. The combined uncertainty (cov. prob. ~95 %) for the evaluation of the amplitude error was evaluated to be lower than 0.1 LSB for the in-phase and 5 LSB for the quadrature component of the output voltage.

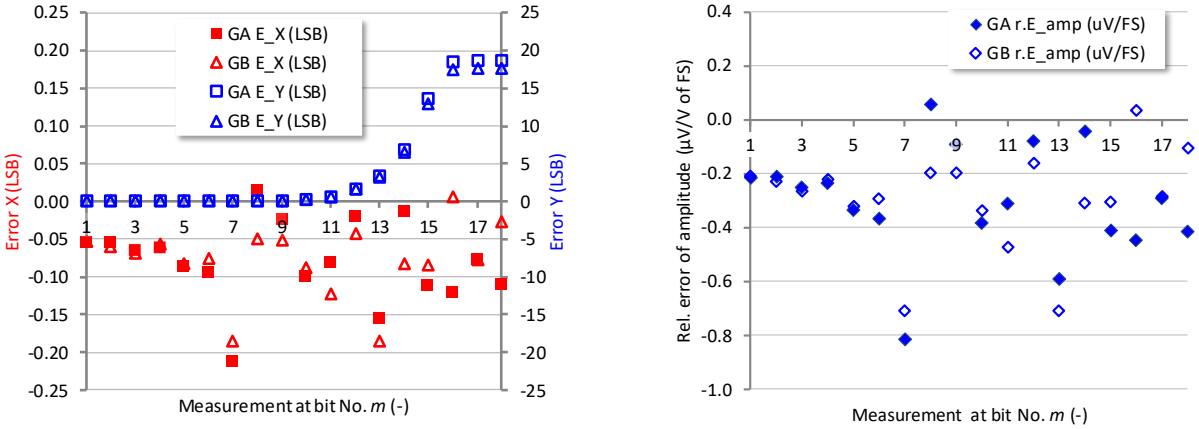

Figure 7. Left: In-phase (E_X) and quadrature (E_Y) voltage errors introduced at 1 kHz in the generator outputs A and B, when programmed word in the mDAC is changed from a1[1:*m*-1]+a0[*m*:18] to a1[1:*m*]+a0[*m*+1:18] and from b1[1:*m*-1]+b0[*m*:18] to b1[1:*m*]+b0[*m*+1:18], respectively, where a1, b1 denotes binary "1" and a0, b0 denotes binary "0" for channels A and B, respectively. Right: contribution to the relative error of the output voltage amplitude (evaluated from the data in the left graph).

2.3.2 Integral nonlinearity

One approach in linearity testing is to perform a voltage measurement of the SWG output using a digitizer with known linearity, where the total rms value or only the amplitude of the first harmonic is evaluated. For the evaluation of the first

harmonic amplitude, a digital multimeter (DMM) Agilent 3458A[1] in DCV sampling mode [17] was used. Nonlinearity in relative form and related to FS voltage is equal to $(U_m–U_s)/U_{FS}$, where U_m denotes the measured voltage, U_s the configured voltage and U_{FS} is FS voltage. While we investigate only the linearity of SWG in this task, we do not need to take care of the absolute accuracy of DMM, only its linearity. We assume that our specific DMM has similar properties as published investigations on other DMMs of the same type. Josephson AC voltage sources have been used to check their linearity as a function of aperture time, e.g. in [16], [24]. For an aperture time of 80 µs, we assume the integral nonlinearity of our DMM to be better than 10 µV/V in the 10-V range for voltages between at least 0.1and 1 of FS (in our case FS=10 V_p). The results are shown in Figure 8 and indicate, that the integral nonlinearity of the SWG for the range from 1 mV_{rms} up to 7 V_{rms} (i.e. from 0.01 % up to 100 % of FS) is smaller than 2 µV/V of FS. The reference transfer function for the integral nonlinearity has a conventional end-point gain correction.

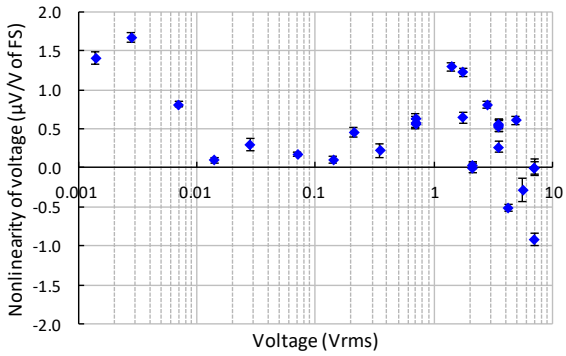

Figure 8. Integral nonlinearity of the output voltage on channel A at a frequency of 1 kHz, relative to the FS voltage. The error bars correspond to the type A uncertainty with coverage probability of ~95%.

3. The generator as a signal source for digital impedance bridges

Generators have been used in NMIs in two types of digital bridges, so called fully digital (FD) and digitally assisted (DA) bridges. Here, we shortly summarize principles of bridges published in [8], [10], [11], where generators have been involved, followed by demonstration of real applications.

3.1 Fully digital bridge

Figure 9 shows a principle scheme of a possible arrangement of a fully digital bridge for a ratio measurement of impedances Z_A and Z_B like 4-TP impedances, which takes advantage of highly stable generators. Details are given in [8]. The ratio of two impedances Z_A and Z_B is proportional to output voltages of channel G2-A and G2-B of a reference generator:

$$Z_B / Z_A \approx U_{G–B} / U_{G–A}. \qquad (1)$$

[1] Commercial instruments are identified in this paper in order to adequately specify the experimental setup and does not imply recommendation or endorsement by the authors.

In accordance with 4-TP definition, zero currents should flow through the high potential arms of Z_A, Z_B. Hence, measuring current through Z_A and Z_B is energized from current arms formed by G3-A and G3-B, which are tuned until zero voltage is detected at points D3 and D4. To fulfill another 4-TP definition, where voltage between inner and outer of LP port should be zero, G2-B is tuned until voltage at Z_B LP port is negligible (point D1). The voltage drop between points D1 and D2 is maintained at a negligible level by means of the injection circuit TR3 with generator G4-B, i.e., voltage at Z_A LP port is maintained at negligible voltage too. All measurement points D*i* (*i*=1, …, 4) are connected to a lock-in amplifier (LIA) via a coaxial multiplexer. LIA is synchronized from the generator G1-A. Typical achievable relative uncertainty of such bridge is on the 10^{-5} level, for 1:1 ratio measurements on 10^{-6} level. An additional injection circuit consisting of the transformer TR4 and the generator G4-A enables users to perform ratio measurements with a fully digital bridge with relative uncertainties down to the 10^{-7} level.

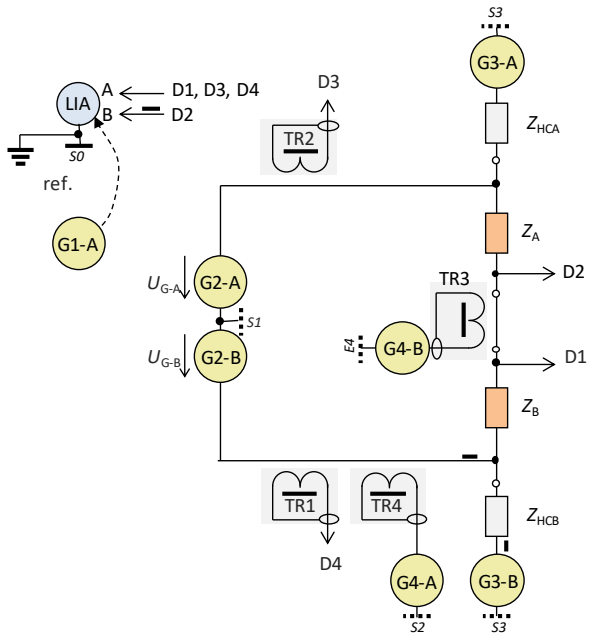

Figure 9. Principle scheme of a fully digital bridge. For simplicity, coaxial wiring is not shown; black rectangles mean coaxial chokes. Same numbers *i* at points *Si* denote grounding points, which are common for paired channels A and B.

For fully digital bridges the stability of multiple generators outputs, synchronized together with a null detector, is crucial. An example of the stability of the impedance ratio measurement *N*=10:1 of Andeen-Hagerling 100 pF and 10 pF AH11[1] capacitors is given in Figure 10. AH11 capacitors were chosen for their excellent stability. Hence, the obtained ratio results correspond mainly to the properties of the investigated generators, especially to relative voltage ratio stability of channels A and B of each SWG module. An Allan deviation analysis of the relative 10:1 ratio going below the level of 10^{-7} demonstrates what can be achieved within one minute. Within 30 minutes, the level of nearly 10^{-8} is reached. Stability of the whole impedance bridge practically confirmed properties of generators, investigated in section 2.2.

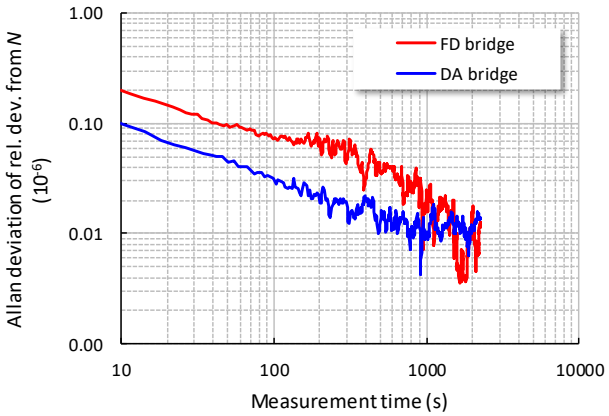

Figure 10. Allan deviation of an N=10:1 ratio measurement using 100 pF and 10 pF capacitors at a frequency of 976 Hz. The bridge voltage for the DA bridge was 1.1 Vrms, and 3.5 Vrms for the FD bridge.

3.2 Digitally assisted bridge

In the comparison with the fully digital bridge described in Figure 9, the reference voltage ratio in the DA bridge is formed by means of an inductive voltage divider, which shows significantly higher long– and shorterm stability than the DDS generators. The DA bridge is built from the FD bridge described above by a simple modification of the bridge circuit. Details are given [8]. A similar Allan deviation analysis for DA and FD bridges in Figure 10 shows good stability of four SWG modules, involved in the bridge circuits. In the FD bridge, a higher noise level was present and the stability of the auxiliary balances probably influences the stability near end of measurement at 2000 s.

3.3 AC QHR bridges

For measuring quantum Hall resistances (QHRs) in the AC regime [13] and work on the realization of AC quantum impedance standard [14], a DA type bridge has been used at CMI, see [11] for details. With a help of non-continuous changes of the sinewave signals in all synchronized generators, a plateau shape in AC regime, a longitudinal resistance, and a frequency dependence of GaAs based QHR device were investigated. With the digital bridge, a basic characterization of double-shielded GaAs based devices can be performed, and the value of quantum Hall resistance can be measured with an uncertainty of few parts in 10^{-8} at the frequency of 1 kHz. Finally, we have shown there, that with proper handling, nearly flat plateau centers could be observed at frequencies from 1 to 4 kHz even at temperature 4.2 K. In the latest, work on the application of FD bridge for the direct capacitance to resistance traceability chain is ongoing [15].

3.4 Sampling type bridge

Authors have not tried it yet, but generators can be simply involved in a sampling type bridge [1] too. Even digitizers with an internal clock of frequency 20 MHz (like DMM 3458A in DCV mode) can be connected without any external synchronization circuits: DMM's 20 MHz output can be used directly as a reference clock for SWG and SWG Sync out can be used for triggering DMM.

In the sampling type bridge, digitizer input has to be switched between different measurement points with a multiplexer. Control signal for switching of such multiplexer can be driven from another SWG module, configured with sufficiently low frequency to achieve required time of digitizing at each measurement point.

4. The generator as a transfer standard for AC quantum voltmeter on-site comparisons

The main parameters for an ideal AC source to be used as a transfer standard for on-site inter-comparisons of quantum voltage standards were listed in previous work [19], [20]. Ideally, the source should provide rms voltages from 10 mV to 7 V, for frequencies ranging from 10 Hz to 2 kHz. The amplitude needs to be stable at least over one set of measurements in the comparison. Phase noise and jitter at its output also affect the repeatability of the results and should be as low as possible. To avoid significant differences in the portions of the period that are sampled by the two systems frequency spectra should be as pure as possible and glitches should be filtered out [23].

PTB has investigated the SWG generator as such a transfer standard for on-site comparisons. In Figure 11 the measurement setup including the synchronization scheme for the AC quantum voltmeter and the synthesizer is shown. Details of the AC quantum voltmeter have been published see e.g. [21], [22]. The sampler measures the difference waveform between the output of the SWG and a stepwise approximated "copy" from the programmable Josephson voltage standard. As the two waveforms are synchronized, the rms amplitude of the SWG output can be calculated from the reconstructed waveform. As the amplitudes at the input of the sampler are kept low, the influence of the sampler errors on the rms measurement of the SWG output is greatly reduced.

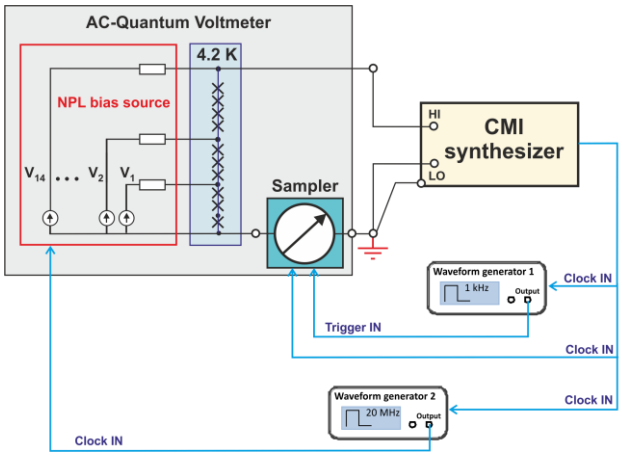

Figure 11. Measurement setup for the characterization of the CMI synthesizer. The blue (dotted) lines show the synchronization signals.

As described above the spectral purity and the absence of glitches is crucial for sampling measurements. If one of these essential characteristics are missing, different sampling parameters will provide different results and comparisons between different sampling systems or thermal transfer devices cannot be performed at the highest level of uncertainty.

Lee et al. [23] have introduced a method to measure the complete curve by sampling a full period in several steps. An equivalent evaluation of glitches and remaining steps in the output waveform can be performed by changing the phase angle between the waveform being measured and the Josephson stepwise approximated copy. As the phase angle changes, different portions of the period are used for the measurement of the rms value. The results of such investigation are depicted in Figure 13. The visible variation of the rms values with phase for channel 1 (CH1, ≈10 µV/V per degree) and channel 2 with buffer and RC filter (≈4 µV/V per degree) clearly indicate that harmonics and glitches are an issue for the synthesizer. However, the graph also clearly shows that the LC filter can reduce such dependence bellow 1 µV/V per degree.

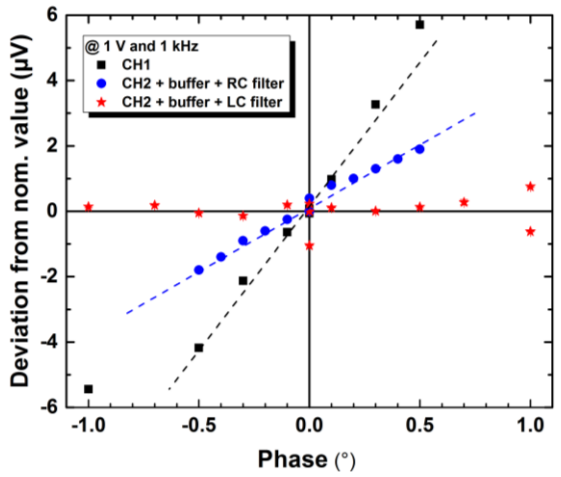

Figure 13. Phase variation with three different output configurations for f = 976.5625 Hz and V_{RMS} = 1 V.

The drawback of using the LC filter is visible in the Allan deviation analysis (see Figure 12), while any additional filter introduces further instability. The minimum of the Allan deviation at 5×10^{-8} is already reached after 10 – 30 s and the level of 10^{-7} after 300 s which would be excellent for an AC voltage transfer device in on-site quantum voltage comparisons. We have further analyzed the stability of the filter by repeating measurements, as shown in Figure 14 on the left side. If we correct for this drift the previous phase measurements, voltage variations remain within 0.1 µV/V for ± 0.5° phase variation (Figure 14 on the right side).

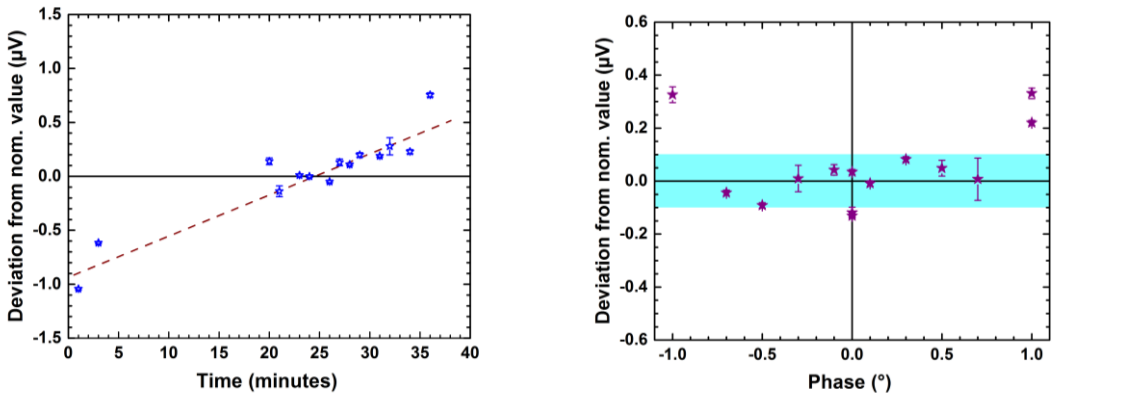

Figure 14. Left: Time trace for f = 976.5625 Hz and V_{RMS} = 1 V phase measurements using the synthesizer output CH2 + buffer + LC filter configuration. Right: Phase dependence for the drift -corrected CH2 + buffer + LC filter configuration. The shaded area indicates the ± 0.1 µV-range.

5. Conclusion

The metrological properties of the sine-wave generator SWG developed at CMI were discussed. Experimental results have shown that it can be a universal tool for building primary impedance calibration setups. Its stability, resolution, spectral purity, synchronization options, output ranges, and optional battery operation have led to digitally assisted impedance bridges with a relative uncertainty down to parts in 10^8. Fully digital impedance bridges have achieved uncertainties of parts in 10^7 level. For

work with quantum Hall based AC impedance standards, excellent results for the characterization of the Quantum Hall plateaux between 1 kHz and 4 kHz were achieved.

The amplitude linearity of the two channels in one module was better than 2 μV/V of FS, and the short-term stability of the ratio between the two channels was up to 0.01 μV/V over 30 minutes. The long-term stability between different SWG modules was better than 6 μV/V over four years.

In addition to the application in impedance metrology, the suitability of the SWG as a transfer standard for AC quantum voltmeter or Josephson differential sampling on-site inter-comparisons was investigated too. The uncertainty for the measurement of the rms amplitude at 1 V and 1 kHz remained below 0.1 μV/V for measurements of up to one-hour duration. Combined with a simple LC filter, the measured rms value remains independent of the phase angle to the Josephson waveform over 1 degree with uncertainty for the output amplitude of 0.1 μV/V. The LC filter, however, reduced the stability of the output amplitude to three minutes and needs further improvement. Even though there is room to improve the output filter stability, our investigations demonstrate that the CMI generator, together with a dedicated filter, is a promising way for future AC quantum voltmeter comparison at the level of parts in 10^7 (0.1 μV/V) or even better.

Acknowledgements

The authors would like to thank J. Grajciar (CMI) and T. Pavlíček (CMI) for consultations and spectral measurements during development of generators.

This work was supported partly by the Joint Research Projects VersICaL (17RPT04) and AIM QuTE (SIB53). These projects have received funding from the EMPIR programme co-financed by the Participating States and from the European Union's Horizon 2020 research and innovation programme. This work was also partly funded by Institutional Subsidy for Long-Term Conceptual Development of a Research Organization granted to the Czech Metrology Institute by the Ministry of Industry and Trade.

References

[1] Overney F and Jeanneret B 2018 Impedance bridges: from Wheatstone to Josephson *Metrologia* 55 S119

[2] Kozioł M, Kaczmarek J and Rybski R 2019 Characterization of PXI-Based Generators for Impedance Measurement Setups *IEEE Trans. Instrum. Meas* **68** 1806–13

[3] Callegaro L, Galzerano G and Svelto C 2001 A multiphase direct-digital-synthesis sinewave generator for high-accuracy impedance comparison Instrumentation and Measurement, *IEEE Trans. Instrum. Meas* **50** 926–9

[4] Nissilä J, Ojasalo K, Kampik M, Kaasalainen J, Maisi V, Casserly M, Overney F, Christensen A, Callegaro L, D'Elia V, Tran N T M, Pourdanesh F, Ortolano M, Kim D B, Penttilä J and Roschier L 2014 A precise two-channel digitally synthesized AC voltage source for impedance metrology *CPEM 2014 Conf. Digest* pp 768–769

[5] Zhuang Y, Magstadt B, Chen T and Chen D 2018 High-Purity Sine Wave Generation Using Nonlinear DAC With Predistortion Based on Low-Cost Accurate DAC–ADC Co-Testing *IEEE Trans. Instrum. Meas* **67** 279–87

[6] Lee J, Schurr J, Nissila J, Palafox L, Behr R and Kibble B P 2011 Programmable Josephson Arrays for Impedance Measurements *IEEE Trans. Instrum. Meas* **60** 2596–601

[7] Cutkosky R 1964 Four-terminal-pair networks as precision admittance and impedance standards *IEEE Trans. Commun. Electron.* **83** 19–22

[8] Kučera, J. and Kováč, J. 2018 A Reconfigurable Four Terminal-Pair Digitally Assisted and Fully Digital Impedance Ratio Bridge, *IEEE Trans. Instrum. Meas.* **67**, pp. 1199-1206.

[9] Ortolano M, Palafox L, Kučera J, Callegaro L, D'Elia V, Marzano M, Overney F and Gülmez G 2018 An international comparison of phase angle standards between the novel impedance bridges of CMI, INRIM and METAS *Metrologia* **55** 499–512

[10] Kučera J and Svoboda P 2018 Development of Ac Quantum Hall Measurements at CMI *CPEM 2018 Conf. Digest*

[11] Kučera J, Svoboda P and Pierz K 2019 AC and DC Quantum Hall Measurements in GaAs-Based Devices at Temperatures Up To 4.2 K *IEEE Trans. Instrum. Meas.* **68** 2106–12

[12] Analog Devices: AD9912. [*Online*] [Date: 1.5.2014] http://analog.com. Rev.F

[13] Ahlers F, Jeanneret B, Overney F, Schurr J and Wood B 2009 Compendium for precise ac measurements of the quantum Hall resistance Metrologia 46 R1

[14] Schurr J, Kucera J, Pierz K and Kibble B P 2011 The quantum Hall impedance standard Metrologia **48** 47–57

[15] Kucera J, Svoboda P 2019 *In preparation*

[16] Kurten W G, Mohns E, Behr R, Williams J M, Patel P, Ramm G and Bachmair H 2005 Characterization of a high-resolution analog-to-digital converter with a Josephson AC voltage source *IEEE Trans. Instrum. Meas.* **54** 649–52

[17] Lapuh R 2018 *Sampling with 3458A* (Left Right d.o.o., Ljubljana, Slovenia)

[18] Awan S, Kibble B and Schurr J 2011 *Coaxial Electrical Circuits for Interference-Free Measurements* (The Institution of Engineering and Technology, London, UK)

[19] Nissilä J, Ojasalo K, Kampik M, Kaasalainen J, Mais V, Casserly M, Overney F, Christensen A, Callegaro L, D'Elia V, Tran N T M, Pourdanesh F, Ortolano M, Kim D B, Penttilä J and Roshier L 2014 A precise two-channel digitally synthesized AC voltage source for impedance metrology *CPEM 2014 Conf. Digest* 768-769

[20] Solve S, Bauer M, Behr R, Palafox L, Kim M-S and Rüfenacht A 2018 Towards a BIPM on-site comparison program for AC voltages based on the differential sampling technique *CPEM 2018 Conf. Digest*

[21] Lee J, Behr R, Palafox L, Schubert M, Starkloff M and Böck A C 2013 An ac quantum voltmeter based on a 10V programmable Josephson array *Metrologia* **50** 612–22

[22] Behr R, Kieler O, Lee J, Bauer S, Palafox L and Kohlmann J 2015 Direct comparison of a 1 V Josephson arbitrary waveform synthesizer and an AC quantum voltmeter Metrologia **52** 528 – 537

[23] Lee J, Nissilä J, Katkov A and Behr R 2014 A quantum voltmeter for precision AC measurements *CPEM 2014 Conf. Digest* 732–733

[24] de Aguilar J D, Salinas J, Kieler O F and Caballero R 2018 Characterization of an analog to digital converter frequency response by a Josephson Arbitrary Waveform Synthesizer *Measurement Science and Technology* **30** 035006